Inorg. Chem. **2008**, *47*, 10469−10478

Copper β-Octakis(trifluoromethyl)corroles: New Paradigms for Ligand Substituent Effects in Transition Metal Complexes

Kolle Ekaney Thomas, Ingar H. Wasbotten, and Abhik Ghosh*

Department of Chemistry and Center for Theoretical and Computational Chemistry, University of Tromsø, N-9037 Tromsø, Norway

Received June 17, 2008

The reaction of copper β-octabromo-*meso*-triarylcorrole derivatives with methyl 2,2-difluoro-2-(fluorosulfonyl)acetate has provided four β-octakis(trifluoromethyl)corrole complexes, Cu[$(CF_3)_8$T(*p*-XP)C] (X = F, H, Me, OMe), in moderate yields. The new complexes present a conglomeration of remarkable substituent effects, both steric and electronic. DFT (OLYP/TZP) geometry optimization of Cu[$(CF_3)_8$TPC] (i.e., X = H) indicates a sterically hindered, strongly saddled geometry, with numerous short F···F nonbonded contacts of 2.5−2.9 Å and certain β carbons displaced by over 1.5 Å relative to the mean corrole plane. The CF_3 groups generally appear as quartets in the ^{19}F NMR spectra, with unexpectedly large $^5J_{FF}$ coupling constants of about 14 Hz, apparently a manifestation of the highly crowded structure. The eight CF_3 groups together exert a powerful influence on the redox potentials of the copper corrole core. Thus, the $E_{1/2ox}$ of Cu[$(CF_3)_8$TPC] (1.4 V vs saturated calomel electrode) is a full half of a volt above that of Cu(TPC) (0.9 V) and a quarter of a volt above that of Cu(Br_8TPC) (1.14 V). Intriguingly, the β CF_3 groups also greatly intensify the influence of the meso aryl substituents on the redox potentials, relative to the other Cu[Y_8T(*p*-XP)C] series, where Y = H, F, and Br. The Cu[$(CF_3)_8$T(*p*-XP)C] complexes also exhibit the most red-shifted optical spectra of any series of metallocorroles synthesized to date. Thus, between Cu(TPC) and Cu[$(CF_3)_8$T(*p*-MeO-P)C], the Soret maximum shifts by nearly 100 nm. The observed red-shifts are attributed in part to charge-transfer transitions of the Soret region and in part to the extreme nonplanar distortions.

Introduction

The chemistry of corroles has grown enormously in recent years, thanks to the availability of convenient one-pot syntheses based on pyrrole−aldehyde condensations.[1,2] Already, the coordination chemistry of corroles promises to rival that of porphyrins, and applications of metallocorroles as transition-metal-containing reagents and catalysts and as novel functional materials are well underway.[3,4] Despite broad similarities, however, there are fundamental differences between porphyrin and corrole chemistry. First, unlike dianionic porphyrins, corrole ligands are typically trianionic and form a completely different set of complexes, which are formally high-valent, relative to stable metalloporphyrins. A second major difference has to do with the inherently lower symmetry of the corrole macrocycle compared with porphyrin—C_{2v} versus D_{4h}. From a materials point of view, the higher symmetry of typical porphyrins implies that they are primarily suitable for third-harmonic generation and related processes that are cubic in the external field.[5,6] In contrast, corroles have a permanent dipole moment and, therefore, should allow for quadratic nonlinear responses.[7] These potential applications provide a strong argument for continued development of the corrole field, particularly for the synthesis of novel substituted corroles.

Over the past few years, we have synthesized a fair number of meso-substituted corrole derivatives, initially to investigate

* Author to whom correspondence should be addressed. E-mail: abhik@chem.uit.no.

(1) (a) Gross, Z.; Galili, N.; Saltsman, I. *Angew. Chem., Int. Ed.* **1999**, *38*, 1427–1429. (b) Paolesse, R.; Mini, S.; Sagone, F.; Boschi, T.; Jaquinod, L.; Nurco, D. J.; Smith, K. M. *Chem. Comm.* **1999**, 1307–1308. (c) Koszarna, B.; Gryko, D. T. *J. Org. Chem.* **2006**, *71*, 3707–3717.

(2) (a) Ghosh, A. *Angew. Chem., Int. Ed.* **2004**, *43*, 1918–1931. (b) Gryko, D. T. *Eur. J. Inorg. Chem.* **2002**, *173*, 5–1743.

(3) Aviv, I.; Gross, Z. *Chem. Comm.* **2007**, 1987–1999.

(4) Gross, Z.; Gray, H. B. *Comments Inorg. Chem.* **2006**, *27*, 61–72.

(5) Albert, I. D. L.; Marks, T. J.; Ratner, M. A. *Chem. Mater.* **1998**, *10*, 753–762.

(6) Cariati, E.; Pizzotti, M.; Roberto, D.; Tessore, F.; Ugo, R. *Coord. Chem. Rev.* **2006**, *250*, 1210–1233.

(7) Misra, R.; Kumar, R.; Prabhu Raja, V.; Chandrashekar, T. K. *J. Photochem. Photobiol. A* **2005**, *175*, 108–117.

10.1021/ic801101k CCC: $40.75
Published on Web 10/18/2008

the generality of one-pot corrole syntheses,[2] but subsequently also to carry out in-depth studies of substituent effects in metallocorroles.[8−10] In particular, we have synthesized a series of β-octafluoro-*meso*-triarylcorroles and their Cu and FeCl complexes[11] with different para substituents on the *meso*-phenyl groups, whose spectroscopic and electrochemical properties provided a host of electronic and structural insights. The recent synthesis of a copper(II) β-octakis(trifluoromethyl)-*meso*-tetraphenylporphyrin[12] via palladium-catalyzed trifluoromethylation of the corresponding β-octabromo complex suggested that analogous β-octakis(trifluoromethyl)metallocorroles should also be attainable, which indeed proved to be the case, as described below. Herein, we report a series of four new copper β-octakis(trifluoromethyl)-*meso*-tris(*p*-X-phenyl)corrole complexes, Cu[$(CF_3)_8$T(*p*-XP)C], where X = F, H, Me, and OMe. Not surprisingly, in view of the eight highly electron-withdrawing trifluoromethyl groups, electrochemical studies have shown that these complexes are among the most electron-deficient metallocorroles known. In the same vein, electronic absorption spectra have also revealed astonishingly large substituent effects. In addition, ^{1}H and ^{19}F NMR spectroscopy and a preliminary density functional theory (DFT) study provide a number of interesting insights into the geometric and electronic structures of these complexes.

Results and Discussion

a. ^{1}H and ^{19}F NMR Spectroscopy. Besides providing a confirmation of structure (in conjunction with the other analytical methods), NMR spectroscopy has provided a number of critical insights into the electronic structure and conformation of the copper corroles studied. For a number of copper corroles, temperature-dependent ^{1}H NMR spectroscopy has indicated the presence of a thermally accessible paramagnetic excited state that is probably best described as $Cu^{II}(Cor^{\bullet 2-})$.[13,14] However, for most of the Cu[$(CF_3)_8$T(*p*-XP)C] complexes examined, the ^{1}H NMR spectra (Figure 1, see also the Supporting Information) remained unchanged and sharp from −40 to +40 °C, indicating a diamagnetic, so-called Cu(III) ground state.

The ^{19}F NMR spectra (Figure 2, see also the Supporting Information), again essentially temperature-independent, turned out to be quite surprising. Given that the CF_3 groups occur as vicinal pairs, we expected to see at best weak $^5J_{FF}$ couplings. Instead, the CF_3 groups appear to be quartets (when they are fully resolved) with unusually large coupling constants of 9−14 Hz. Figure 2 depicts key regions of the ^{19}F NMR spectrum of Cu[$(CF_3)_8$TPC] as well as the ^{19}F−^{19}F COSY. Note that two CF_3 pairs appear as distinct quartets at −50.78 (J = 14.3 Hz) and −55.11 (J = 12.0 Hz) ppm, whereas the other two CF_3 pairs appear to overlap partially, leading to a muliplet located between −51.30 and −51.56 ppm. However, careful examination of the multiplet, which integrates to double the area of either of the two clear quartets, indicates that it results from two partially overlapping quartets at approximately −51.39 and −51.47, with J values of approximately 12.0 and 14.3 Hz, respectively. The ^{19}F−^{19}F COSY reveals that the peak clusters centered at −51.39 and −55.11 ppm couple with each other, as do the peak clusters centered at −50.78 and −51.47 ppm. The pairs of mutually coupling peak clusters appear to be assignable to vicinal pairs of CF_3 groups; however, a more detailed assignment has not yet proved possible. Interestingly, in contrast to the clear evidence for large inter-CF_3 $^5J_{FF}$ couplings, there is no evidence for intra-CF_3 $^2J_{FF}$ coupling, indicating that the CF_3 groups, though congested, are still rotating freely on the NMR time scale. In the same vein, the ortho and meta protons of the 5,15 aryl groups appear as single signals, rather than as diastereotopic pairs, as they would in a static saddled structure. Given the steric crowding, saddling inversion, rather than free aryl rotation, appears to provide the most likely mechanism for the equivalence (diastereotopomerization) of the ortho (or meta) protons on each aryl ring.

Moderate long-range $^4J_{FF}$ couplings are well precedented for perfluoroisopropyl groups.[15] Of the many relevant compounds in the literature, the most pertinent appears to be perfluoro(6-isopropyl-2,4,5-trimethylbenzonitrile), where an inter-CF_3 $^5J_{FF}$ coupling of 4 Hz was observed.[16] In recent years, Strauss and co-workers have also reported a number of fluorinated and trifluoromethylated fullerene derivatives, a number of which also exhibit long-range F−F coupling.[17]

b. DFT Calculations.[18,19] Nearly every aspect of the complexes synthesized is an attractive topic for theoretical analysis. To limit the scope of this study, therefore, we have chosen to focus on the issue of molecular structure and conformation. Unfortunately, none of the four complexes synthesized lent themselves to X-ray crystallographic analysis, so DFT geometry optimizations,[20] which have generally performed well for other high-valent copper tetrapyrroles,[21−23] were performed to shed light on the question of structure and conformation. Figure 3 depicts highlights of an OLYP[24]/STO-TZP optimized geometry of Cu[$(CF_3)_8$TPC] as well as, for comparison, the structures of Cu[Br_8TPC] and the corresponding porphyrin derivatives Cu^{II}[Y_8TPP] (Y = CF_3, Br). The optimized structures afford a variety of insights.

Perhaps the most notable feature of the optimized geometry of Cu[$(CF_3)_8$TPC] (Figures 3a) is that it is severely nonplanar — saddled — much more so than Cu(Br_8TPC), for example (Figure 3b).[25] Thus, two of the four symmetry-

(8) Steene, E.; Wondimagegn, T.; Ghosh, A. *J. Phys. Chem. B* **2001**, *105*, 11406–11413, Addition/correction: *J. Phys. Chem. B* **2002**, *106*, 5312−5312.
(9) Wasbotten, I. H.; Wondimagegn, T.; Ghosh, A. *J. Am. Chem. Soc.* **2002**, *124*, 8104–8116.
(10) Albrett, A. M.; Conradie, J.; Boyd, P. D. W.; Clark, G. R.; Ghosh, A.; Brothers, P. J. *J. Am. Chem. Soc.* **2008**, *130*, 2888–2889.
(11) Steene, E.; Wondimagegn, T.; Ghosh, A. *J. Am. Chem. Soc.* **2003**, *125*, 16300–16309.
(12) Liu, C.; Chen, Q.-Y. *Eur. J. Org. Chem.* **2005**, 3680–3686.
(13) Brückner, C.; Brinas, R. P.; Bauer, J. A. K. *Inorg. Chem.* **2003**, *42*, 4495–4497.
(14) Luobeznova, I.; Simkhovich, L.; Goldberg, I.; Gross, Z. *Eur. J. Inorg. Chem.* **2004**, *8*, 1724–1732.
(15) Chambers, R. D.; Sutcliffe, L. H.; Tiddy, G. J. T. *Trans. Faraday Soc.* **1970**, *66*, 1025–1038.
(16) Batsanov, A. S.; Richmond, P.; Sandford, G.; Chambers, R. D. *Acta Crystallogr., Sect. E* **2005**, *61*−O46.

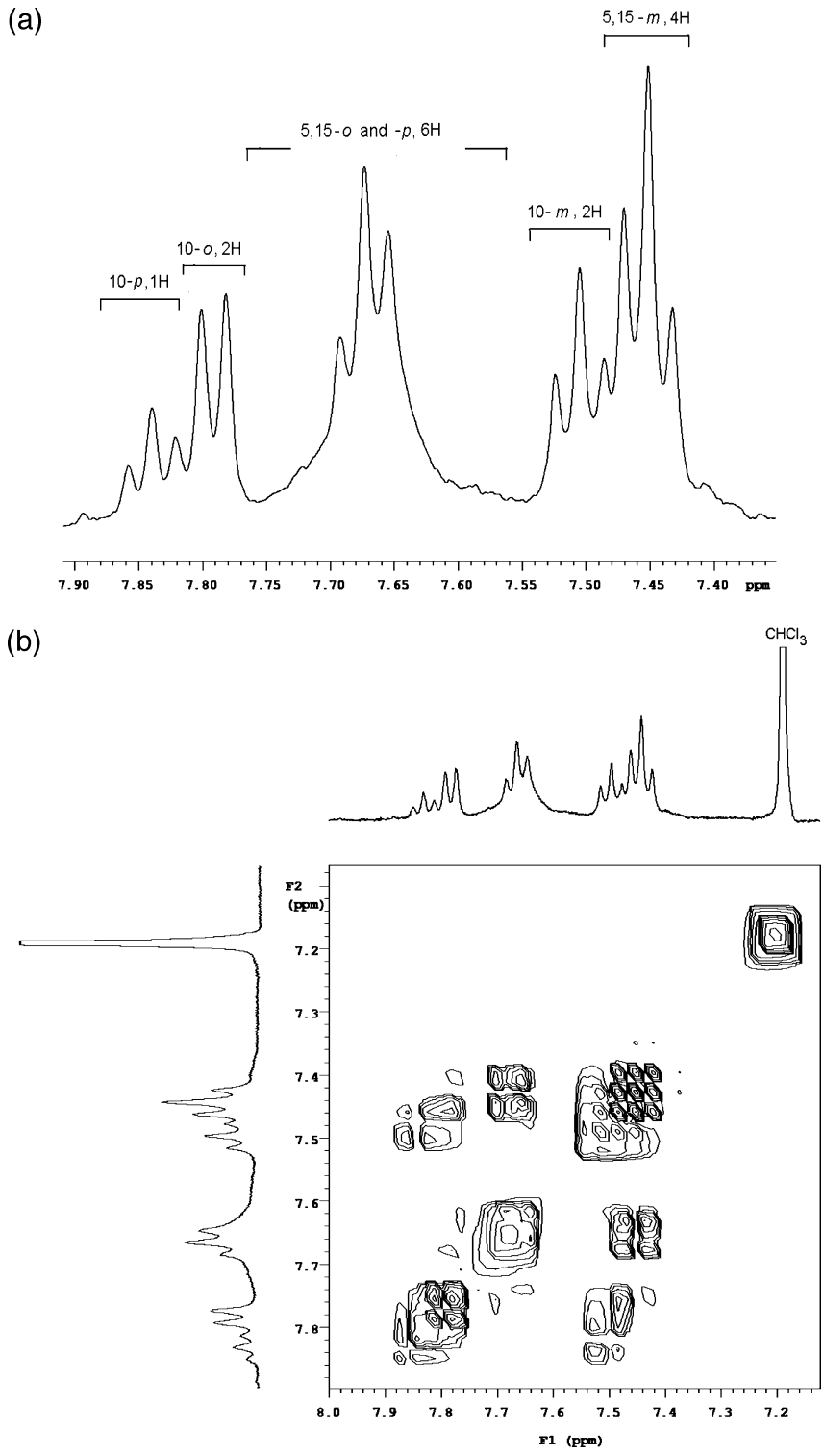

Figure 1. The ^{1}H NMR spectrum and ^{1}H−^{1}H COSY of Cu[$(CF_3)_8$TPC]: (a) the 1D spectrum and (b) the ^{1}H−^{1}H COSY.

distinct β carbons of Cu[$(CF_3)_8$TPC] are displaced by over 1.5 Å relative to the mean corrole plane, which is unprecedented for any corrole derivative synthesized to date. The other two symmetry-distinct β carbons are displaced less, but still by over 1.0 Å, relative to the same plane. Although these β-carbon displacements are slightly smaller than those in Cu^{II}[$(CF_3)_8$TPP], they are considerably higher than those calculated for Cu(Br_8TPC). As shown in Figure 3a, the highly congested structure of Cu[$(CF_3)_8$TPP] results in numerous very short F···F nonbonded contacts of 2.5−2.9 Å, providing a qualitative rationale for the strong $^5J_{FF}$ couplings described above.

The calculations provide limited insight into the question of the metal oxidation state in the complexes in question. The Cu−N distances in Cu[$(CF_3)_8$TPC] are about 0.05 Å shorter than those in the Cu(II) porphyrin analogue, consistent with a d^8 Cu(III) configuration in the corrole case. However, although pure functionals such as OLYP (as well

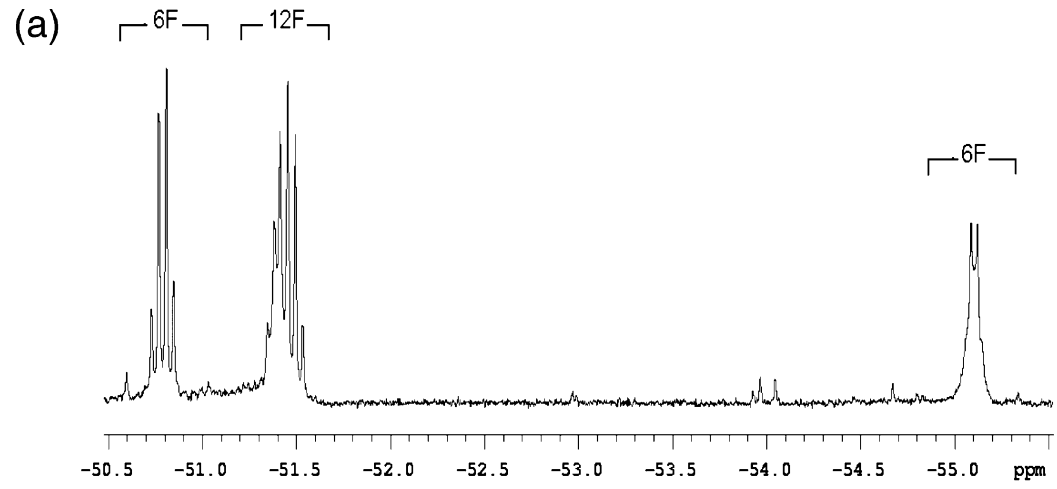
(a)
6F
12F
6F
-50.5
-51.0
-51.5
-52.0
-52.5
-53.0
-53.5
-54.0
-54.5
-55.0
ppm

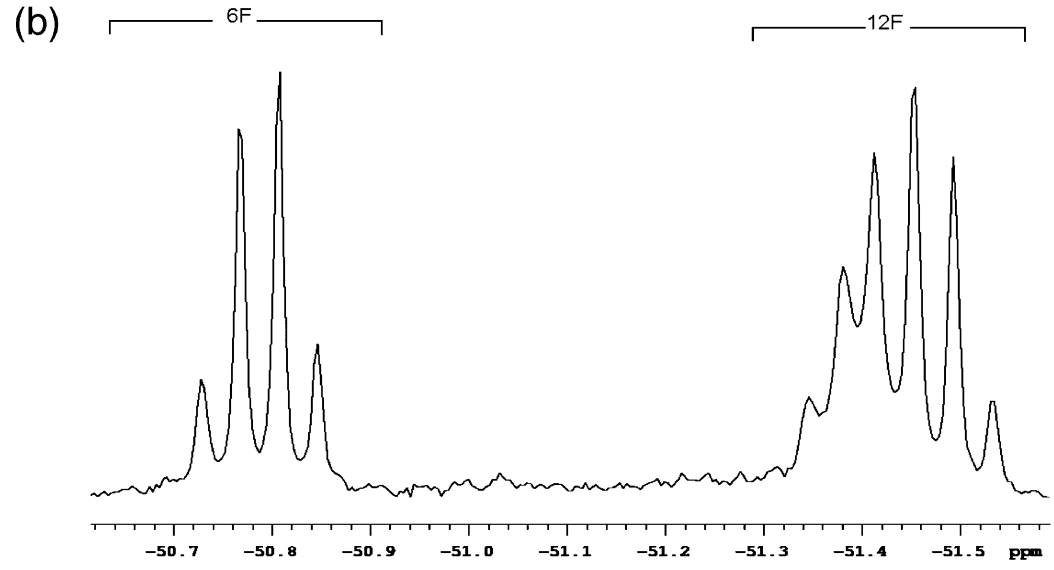
(b)
6F
12F
-50.7
-50.8
-50.9
-51.0
-51.1
-51.2
-51.3
-51.4
-51.5
ppm

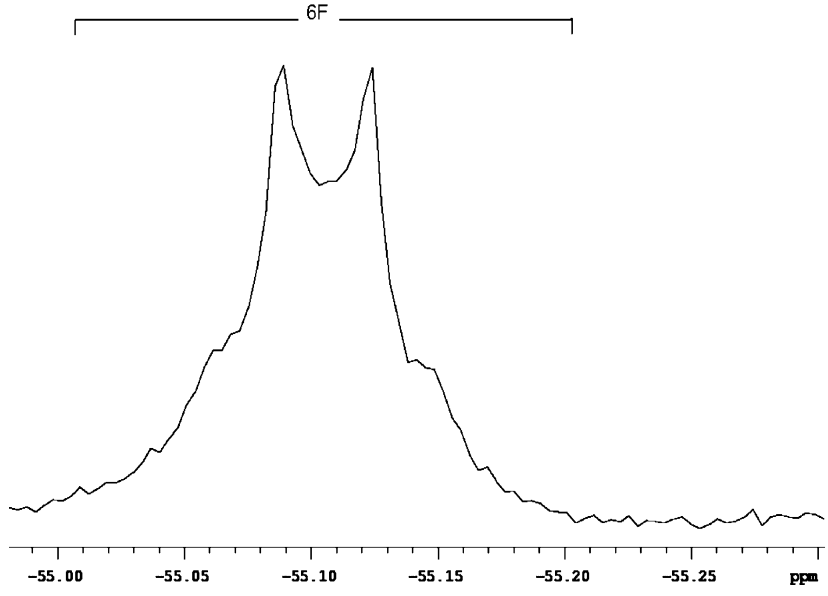
6F
-55.00
-55.05
-55.10
-55.15
-55.20
-55.25
ppm

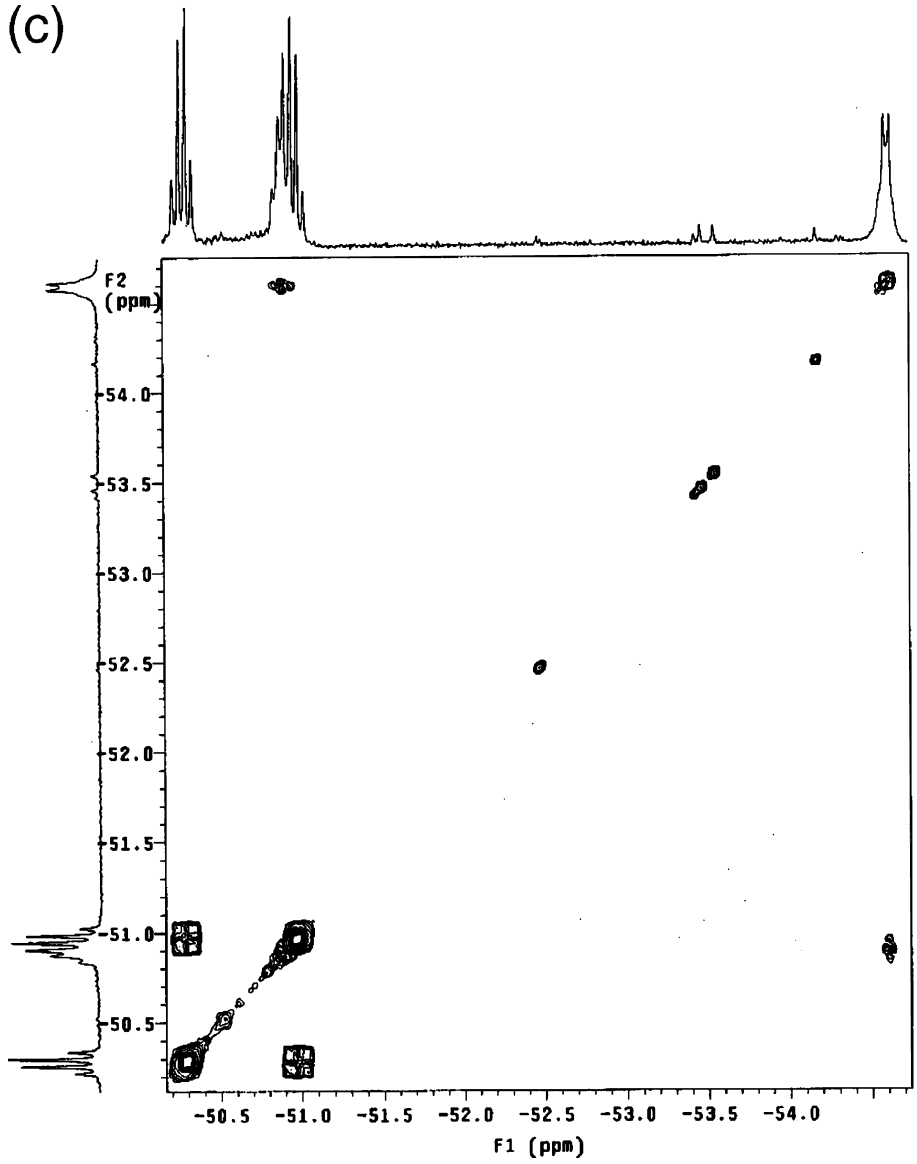

Figure 2. ^{19}F NMR spectra of Cu[$(CF_3)_8$TPC]: (a) the full range, (b) expanded views of the peaks, and (c) the $^{19}F-^{19}F$ COSY.

as PW91, BP86, and BLYP) provide an essentially covalent, perfectly spin-coupled description of the Cu−N bonding, B3LYP results in modest spatial separation of the α and β spin densities, arguing for a certain amount of Cu(II) $Cor^{\bullet 2-}$ character. The effect is qualitatively similar to that reported recently for another, more moderately saddled copper corrole complex.[26]

c. Electrochemistry. On the basis of a large body of previous work,[8,9,27,28] the two observed redox processes in the cyclic voltammogram of each complex (Figure 4) appear to be safely assignable to the following half-reactions:

$$\{Cu[(CF_3)_8T(p\text{-}XP)C]\}^+ + e^- \rightarrow Cu[(CF_3)_8T(p\text{-}XP)C] \quad E_{1/2ox} \quad (1)$$

$$Cu[(CF_3)_8T(p\text{-}XP)C] + e^- \rightarrow \{Cu[(CF_3)_8T(p\text{-}XP)C]\}^- \quad E_{1/2red} \quad (2)$$

The measured redox potentials are listed in Table 1, along with those of other comparable series of metallocorroles with different para substituents on the *meso*-aryl groups. The eight β-CF_3 groups clearly exert a dramatic influence on both $E_{1/2ox}$ and $E_{1/2red}$. Thus, the $E_{1/2ox}$ of Cu[$(CF_3)_8$TPC] is a full half of a volt above that of Cu(TPC) and a quarter of a volt above that of Cu(Br_8TPC). The effect of the β-CF_3 groups on the $E_{1/2red}$ is somewhat different. While the $E_{1/2red}$ of Cu[$(CF_3)_8$TPC] is nearly half of a volt (460 mV) higher than that of Cu(TPC), it is only 0.1 V or less higher than that of either Cu(Br_8TPC) or Cu(F_8TPC). In other words, whereas β F, Br, and CF_3 groups result in roughly comparable stabilizations (in energy terms) of the anionic $\{Cu[Y_8T(p\text{-}XP)C]\}^-$ (Y = F, Br, CF_3) states, the β-CF_3 groups destabilize the corresponding $\{Cu[Y_8T(p\text{-}XP)C]\}^+$ cations far more drastically than F or Br substituents. A simple explanation for this difference is that, although halogens are net electron-withdrawing substituents, they stabilize carbocations via mesomeric electron donation, which is out of the question for CF_3 substituents. We can thus understand the exceptional instability of the $\{Cu[(CF_3)_8T(p\text{-}XP)C]\}^+$ cations.

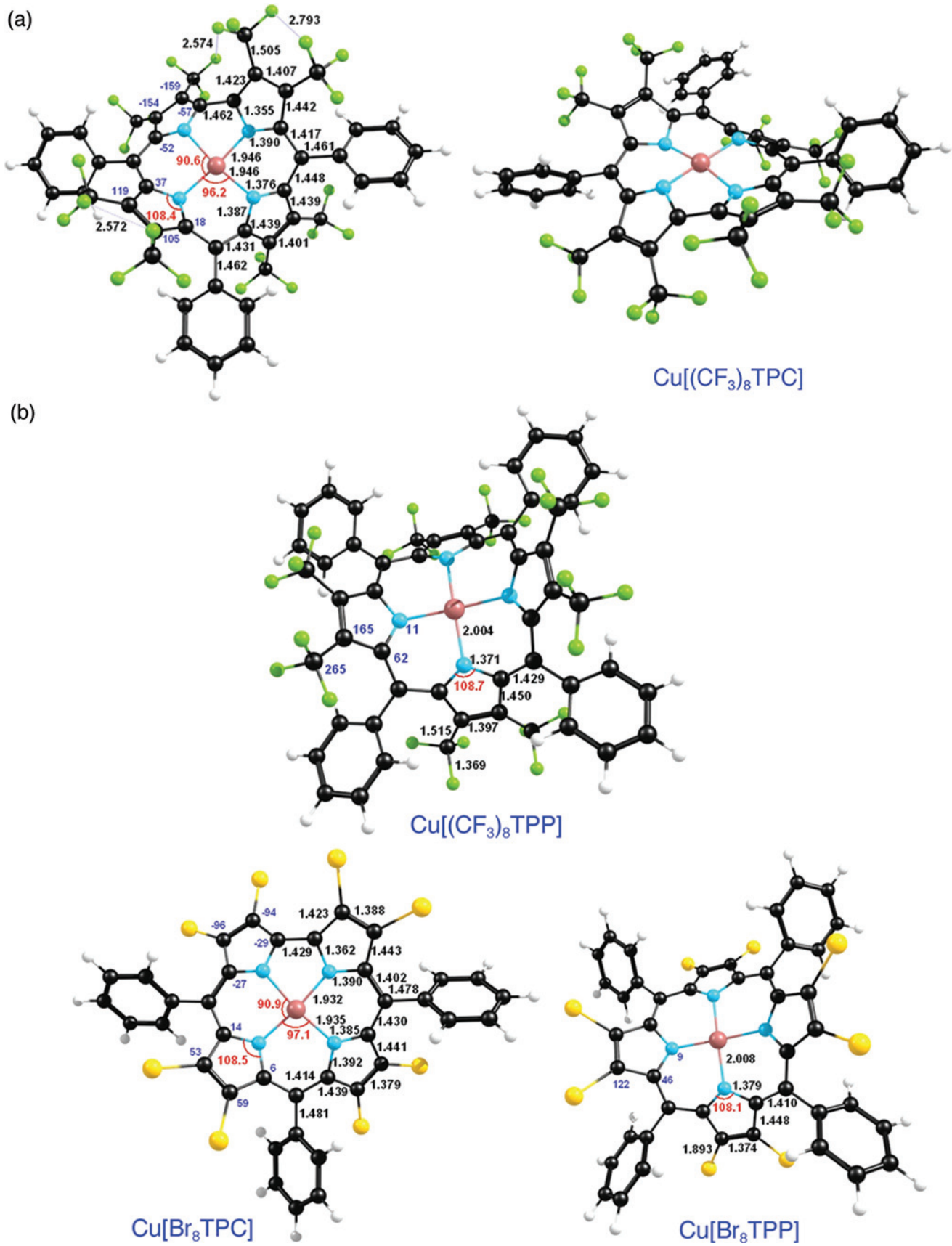

Figure 3. OLYP/TZP optimized geometries of Cu[Y_8TPC] (corroles) and Cu^{II}[Y_8TPP] (porphyrins), where Y = CF_3 and Br. Part a depicts highlights of the Cu[$(CF_3)_8$TPC] geometry as well as a sideways perspective; the other structures are shown in part b. Selected bond distances (Å) and angles (deg) are shown in black and red, respectively. Displacements (pm) of selected atoms relative to the mean corrole plane (which passes through the meso carbons in each structure) are shown in blue. Color code for atoms: C (black), N (cyan), H (ivory), F (darker green), and Br (yellow-orange).

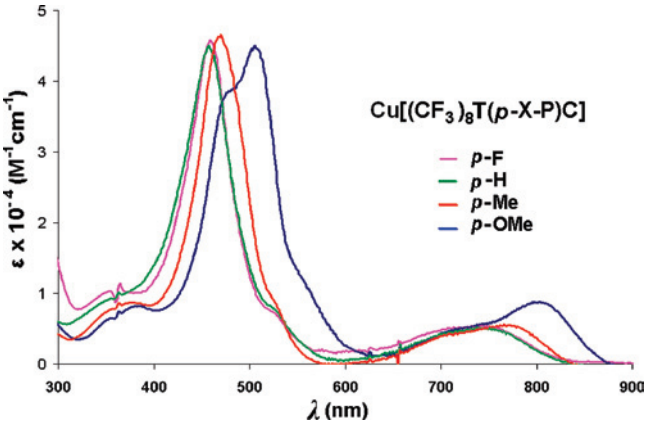

Figure 4. Cyclic voltammograms of the Cu[$(CF_3)_8$T(*p*-XP)C] complexes.

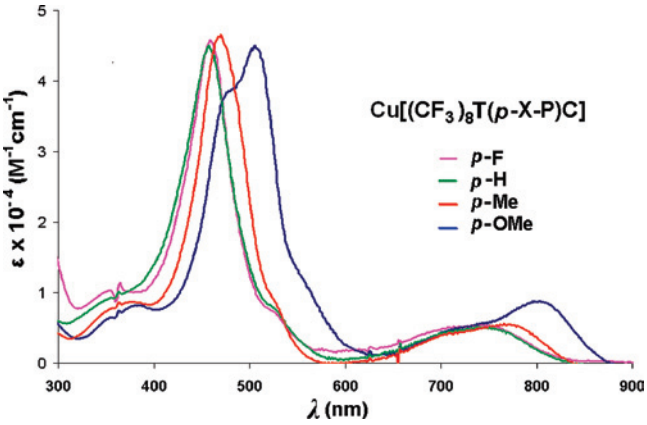

Figure 5. UV−visible spectra of the Cu[$(CF_3)_8$T(*p*-XP)C] complexes in CH_2Cl_2.

Another intriguing feature of the Cu[$(CF_3)_8$T(*p*-XP)C] derivatives is that the β-CF_3 groups appear to dramatically heighten meso substituent effects on both $E_{1/2ox}$ and $E_{1/2red}$, relative to the other series of [Y_8T(*p*-XP)C] complexes, where Y = H, F, and Br. The effect for $E_{1/2ox}$ is particularly intense. Thus, based on the relevant Hammett equation[29]

$$\rho_{ox} = \frac{1}{3}\frac{dE_{1/2ox}}{d\sigma} = 278 \text{ mV} \qquad (3)$$

for the Cu[$(CF_3)_8$T(*p*-XP)C] series is 3−6 times that found for the other series (see Table 1).

d. Electronic Absorption Spectroscopy. The electronic absorption spectra of the four Cu[$(CF_3)_8$T(*p*-XP)C] derivatives are shown in Figure 5. In addition, Table 2 lists the Soret maxima for several families of metallocorroles as a function of the para substituents on the meso aryl groups. Two key generalizations emerge from the results. First, the Cu[$(CF_3)_8$T(*p*-XP)C] complexes exhibit the most red-shifted optical spectra of any series of metallocorroles synthesized to date. Second, meso substituent effects, as measured by shifts in the Soret absorption maximum, are higher in the Cu[$(CF_3)_8$T(*p*-XP)C] series than in any other series of metallocorroles.

Although we have not analyzed the electronic absorption spectra of the Cu[$(CF_3)_8$T(*p*-XP)C] complexes by theoretical means,[30] earlier studies afford a degree of understanding of the present results. DFT calculations[9] on unsubstituted copper corrole revealed a very low-energy Cu $d_{x^2-y^2}$-based LUMO; time-dependent density-functional theory (TDDFT) calculations further indicated strong charge-transfer transitions in the Soret region involving this orbital. The strong substituent sensitivity of the Soret band of the Cu[$(CF_3)_8$T(*p*-XP)C] complexes is consistent with this picture. Note that, in the absence of sufficiently low-energy unoccupied orbitals, as in the case for free-base corroles, the Soret maxima do not shift appreciably as a function of the para substituent on the meso aryl groups. The Soret absorption maxima of the recently reported, anionic diboron corroles, [(FBOBF)T(*p*-XP)C]$^-$, which have electronically saturated boron centers, are similarly insensitive to meso substituent effects.[10] In the same vein, the astonishing 100 nm range of copper triaryl-

Table 1. Half-Wave Potentials vs SCE ($E_{1/2}$, V) and Hammett ρ Values (= 1/3[($dE_{1/2}$)/($d\sigma$)], mV) for MnCl, FeCl, Fe−O−Fe, and Cu *meso*-Triarylcorroles in CH_2Cl_2 Containing 0.1 M TBAP

corrole	X	3σ	$E_{1/2ox}$	$E_{1/2red}$	ρ_{OX}	ρ_{red}	ref
Mn[T(*p*-X-P)C]Cl	CF_3	1.62	1.150	0.230	82	77	8
	H	0	1.032	0.093			
	CH_3	−0.51	0.970	0.072			
Fe[T(*p*-X-P)C]Cl	CF_3	1.62	1.178	0.190	74	77	8
	H	0	1.068	0.050			
	CH_3	−0.51	1.015	0.033			
Fe[F_8T(*p*-X-P)C]Cl	CF_3	1.62	1.47	0.63	49	68	11
	H	0	1.40	0.49			
	CH_3	−0.51	1.38	0.48			
	OCH_3	−0.80	1.34	0.47			
{Fe[T(*p*-X-P)C]}$_2$O	CF_3	1.62	0.830	−0.115	114	109	8
	H	0	0.635	−0.305			
	CH_3	−0.51	0.593	−0.350			
Cu[T(*p*-X-P)C]	CF_3	1.62	0.89	−0.08	95	68	9
	H	0	0.76	−0.20			
	CH_3	−0.51	0.70	−0.23			
	OCH_3	−0.80	0.65	−0.24			
Cu[Br_8T(*p*-X-P)C]	CF_3	1.62	1.24	0.25	58	86	9
	H	0	1.14	0.12			
	CH_3	−0.51	1.12	0.07			
	OCH_3	−0.80	1.10	0.04			
Cu[F_8T(*p*-X-P)C]	CF_3	1.62	1.24	0.35	67	77	11
	H	0	1.15	0.22			
	CH_3	−0.51	1.12	0.18			
	OCH_3	−0.80	1.06	0.17			
Cu[$(CF_3)_8$T(*p*-X-P)C]	**F**	**0.186**	**1.41**	**0.30**	**278**	**160**	this work
	H	**0**	**1.39**	**0.26**			
	CH_3	**−0.51**	**1.29**	**0.18**			
	OCH_3	**−0.80**	**1.12**	**0.14**			

Table 2. Soret Absorption Maxima (nm) of Triarylcorrole Derivatives in CH_2Cl_2[a]

	X					
corrole	F	CF_3	H	CH_3	OCH_3	ref
H_3[T(*p*-X-P)C]	415	417	417	417	421	9
H_3[F_8T(*p*-X-P)C]	−	404	403	405	410	11
[(FBOBF)T(*p*-XP)C]$^-$	−	421	418, 421	415	−	11
Mn[T(*p*-X-P)C]Cl	−	423	433	441	−	8
Fe[T(*p*-X-P)C]Cl	−	402	411	421	−	8
Fe[F_8T(*p*-X-P)C]Cl	−	353	355	360	367	11
{Fe[T(*p*-X-P)C]}$_2$O	−	384	385	389	−	8
Cu[T(*p*-X-P)C]	412	407	413	418	433	9
Cu [Br_8T(*p*-X-P)C]	445	436	439	453	468	9
Cu[F_8T(*p*-X-P)C]	−	401	409	421, 380(sh)	436, 380	11
Cu[$(CF_3)_8$T(*p*-X-P)C]	462	−	**459**	**471**	**507**	**this work**

[a] Note: "−" indicates that the compound in question was not or could not be synthesized.

corrole Soret maxima (see Table 2 for appropriate examples) contrasts sharply with the relative insensitivity of typical Ni(II) or Zn(II) tetraarylporphyrin electronic spectra to variations in the meso aryl group (see, e.g., ref 29).

To what extent do the large Soret red-shifts reflect the strongly saddled geometries of the Cu[$(CF_3)_8$T(*p*-XP)C] complexes? An examination of the recent literature suggests that the arguments involved in answering this question may be rather involved. Thus, although nearly all nonplanar metalloporphyrins exhibit red-shifted optical spectra relative to their planar congeners,[31] TDDFT calculations on unsubstituted metalloporphine derivatives optimized with different degrees of ruffling (i.e., the degree of ruffling is the only constraint in the geometry optimizations) did not reveal any appreciable red-shift of the Soret region.[32,33] The solution to this conundrum is that the ruffling deformation *per se* does not engender significantly red-shifted optical spectra. Instead, higher-energy out-of-plane displacements (i.e., corresponding to higher-frequency out-of-plane normal modes), which are invariably present in sterically hindered, ruffled metalloporphyrins, are the key agents of the spectral red-shifts.[22,34] We would like to postulate that an exactly similar scenario holds for sterically hindered, saddled metalloporphyrins and, by analogy, also for the saddled metallocorroles. According to this view,[35] then, the exceptional Soret red-shifts of the Cu[$(CF_3)_8$T(*p*-XP)C] complexes (relative to their β-unsubstituted analogues), to a significant extent, result from large, substituent-dictated deformations of key dihedral angles involving atoms of the corrole core, as opposed to pure saddling. As mentioned,[30] TDDFT does not appear to be suited for testing this hypothesis; we are currently examining more elaborate quantum chemical schemes for studying this issue.

Conclusion

In conclusion, we have reported the first copper β-octakis-(trifluoro-methyl)corrole complexes, Cu[$(CF_3)_8$T(*p*-XP)C], with systematically varying meso-substituents (X = F, H, Me, OMe). The emphasis has been largely on an experimental study of substituent effects, involving electronic absorption and ^{1}H and ^{19}F NMR spectroscopies as well as from electrochemistry. DFT calculations were invoked largely to illuminate the molecular structures, which, unfortunately, could not be obtained from X-ray crystallography. The substituents exert remarkable effects on both ground- and excited-state properties of the complexes, as summarized below.

(17) (a) Kareev, I. E.; Kuvychko, I. V.; Lebedkin, S. F.; Miller, S. M.; Anderson, O. P.; Seppelt, K.; Strauss, S. H.; Boltalina, O. V. *J. Am. Chem. Soc.* **2005**, *127*, 8362–8375. (b) Kareev, I. E.; Quinones, G. S.; Kuvychko, I. V.; Khavrel, P. A.; Ioffe, I. N.; Goldt, I. V.; Lebedkin, S. F.; Seppelt, K.; Strauss, S. H.; Boltalina, O. V. *J. Am. Chem. Soc.* **2005**, *127*, 11497–11504. (c) Shustova, N. B.; Kuvychko, I. V.; Bolskar, R. D.; Seppelt, K.; Strauss, S. H.; Popov, A. A.; Boltalina, O. V. *J. Am. Chem. Soc.* **2006**, *128*, 15793–15798. (d) Popov, A. A.; Kareev, I. E.; Shustova, N. B.; Stukalin, E. B.; Lebedkin, S. F.; Seppelt, K.; Strauss, S. H.; Boltalina, O. V.; Dunsch, L. *J. Am. Chem. Soc.* **2007**, *129*, 11551–11568.

(18) Reviews on DFT studies of porphyrins and related compounds:(a) Ghosh, A. *Acc. Chem. Res.* **1998**, *31*, 189–198. (b) Ghosh, A. In *The Porphyrin Handbook*; Kadish, K. M., Guilard, R., Smith, K. M., Eds.; Academic: San Diego, CA, 1999; Vol. *7*, Chapter 47, pp 1−38. (c) Ghosh, A.; Steene, E. *J. Biol. Inorg. Chem.* **2001**, *6*, 739–752. (d) Ghosh, A.; Taylor, P. R. *Curr. Opin. Chem. Biol.* **2003**, *91*, 113–124. (e) Ghosh, A. *J. Biol. Inorg. Chem.* **2006**, *11*, 712–724.

(19) DFT studies of corroles and corrole analogues:(a) Ghosh, A.; Jynge, K. *Chem.—Eur. J.* **1997**, *3*, 823–833. (b) Ghosh, A.; Wondimagegn, T.; Parusel, A. B. J. *J. Am. Chem. Soc.* **2000**, *122*, 5100–5104. (c) Bendix, J.; Dmochowski, I. J.; Gray, H. B.; Mahammed, A.; Simkhovich, L.; Gross, Z. *Angew. Chem., Int. Ed.* **2000**, *39*, 4048–4051. (d) Tangen, E.; Ghosh, A. *J. Am. Chem. Soc.* **2002**, *124*, 8117–8121. (e) van Oort, B.; Tangen, E.; Ghosh, A. *Eur. J. Inorg. Chem.* **2004**, 2442–2445. (f) Ghosh, A.; Wasbotten, I. H.; Davis, W.; Swarts, J. C. *Eur. J. Inorg. Chem.* **2005**, *447*, 9–4485. (g) Wasbotten, I.; Ghosh, A. *Inorg. Chem.* **2006**, *45*, 4910–4913.

(20) All DFT calculations were carried out with the ADF 2007 program system using methods described in:(a) Velde, G. T.; Bickelhaupt, F. M.; Baerends, E. J.; Guerra, C. F.; Van Gisbergen, S. J. A.; Snijders, J. G.; Ziegler, T. *J. Comput. Chem.* **2001**, *22*, 931–967.

(21) Bröring, M.; Bregier, F.; Tejero, E. C.; Hell, C.; Holthausen, M. C. *Angew. Chem., Int. Ed.* **2007**, *46*, 445–448.

(22) Parusel, A. B. J.; Wondimagegn, T.; Ghosh, A. *J. Am. Chem. Soc.* **2000**, *122*, 6371.

(23) For other studies on the performance of DFT, vis-à-vis the structures of copper corroles and analogues, see:(a) Wasbotten, I.; Ghosh, A. *Inorg. Chem.* **2006**, *45*, 4914–4921. (b) van Oort, B.; Tangen, E.; Ghosh, A. *Eur. J. Inorg. Chem.* **2004**, *244*, 2–2445.

(24) The OPTX exchange functional, part of the OLYP functional, was reported in:(a) Handy, N. C.; Cohen, A. *J. Mol. Phys.* **2001**, *99*, 403–412.

(25) The strong saddling predicted may be contrasted with the relative planarity of certain other undecasubstituted metallocorroles:(a) Paolesse, R.; Licoccia, S.; Bandolig, A. D.; Boschi, T. *Inorg. Chem.* **1994**, *33*, 1171–1176. (b) Palmer, J. H.; Day, M. W.; Wilson, A. D.; Henling, L. M.; Gross, Z.; Gray, H. B. *J. Am. Chem. Soc.* **2008**, *130*, 7786–7787. The factors responsible for saddling in corroles are still unclear and under active study in our laboratory, both experimentally and with DFT methods. In unpublished work in our laboratory, we have found two *sterically unhindered, β-unsubstituted* Cu triarylcorrole complexes which exhibit moderately saddled geometries, suggesting that Cu(III) corroles may be particularly prone to saddling, relative to other metallocorroles: Alemayehu, A.; Hansen, L. K.; Ghosh, A. Manuscript in preparation.

(26) (a) Bröring, M.; Bregier, F.; Tejero, E. C.; Hell, C.; Holthausen, M. C. *Angew. Chem., Int. Ed.* **2007**, *46*, 445–448. For a review on noninnocent corrole ligands, see: (b) Walker, F. A.; Licoccia, S.; Paolesse, R. *J. Inorg. Biochem.* **2006**, *100*, 810–837.

(27) Ou, Z.; Shao, J.; Zhao, H.; Ohkubo, K.; Wasbotten, I. H.; Fukuzumi, S.; Ghosh, A.; Kadish, K. M. *J. Porphyrins Phthalocyanines* **2004**, *8*, 1236–1247.

(28) Ghosh, A.; Steene, E. *J. Inorg. Biochem.* **2002**, *91*, 423–436.

(29) In our view, a series of four complexes constitutes the smallest set for a legitimate Hammett analysis. For a similar Hammett analysis of β-octahalogenometalloporphyrins, see: (a) Ghosh, A.; Halvorsen, I.; Nilsen, H. J.; Steene, E.; Wondimagegn, T.; Lie, R.; van Caemelbecke, E.; Guo, N.; Ou, Z.; Kadish, K. M. *J. Phys. Chem. B* **2001**, *105*, 8120–8124.

(30) TDDFT calculations had trouble reproducing the observed substituent effects in the Cu[$(CF_3)_8$T(*p*-XP)C] series. This is a well-recognized limitation of common TDDFT schemes: standard exchange-correlation functionals do not correctly describe long-range interelectronic interactions that are involved in charge-transfer transitions.

(31) Shelnutt, J. A.; Song, X.-Z.; Ma, J.-G.; Jia, S.-L.; Jentzen, W.; Medforth, C. J. *Chem. Soc. Rev.* **1998**, *27*, 31.

(32) (a) DiMagno, S. G.; Wertsching, A. K.; Ross, C. R. *J. Am. Chem. Soc.* **1995**, *117*, 8279. (b) Wertsching, A. K.; Koch, A. S.; DiMagno, S. G. *J. Am. Chem. Soc.* **2001**, *123*, 3932–3939.

(33) Ryeng, H.; Ghosh, A. *J. Am. Chem. Soc.* **2002**, *124*, 8099–8103.

(34) Haddad, R. E.; Gazeau, S.; Pecaut, J.; Marchon, J.-C.; Medforth, C. J.; Shelnutt, J. A. *J. Am. Chem. Soc.* **2003**, *125*, 1253–1268.

(35) Though speculative, we believe that our argument is based solidly on literature precedence.[34] The literature on spectral redshifts, vis-à-vis nonplanar distortions, is rather convoluted, and the nonexpert reader may find a useful summary in the section entitled "A Note on the Electronic Absorption Spectra of Nonplanar Porphyrins" in:(a) Wasbotten, I. H.; Conradie, J.; Ghosh, A. *J. Phys. Chem. B* **2003**, *107*, 3613–3623.

1. DFT calculations suggest that copper β-octakis(trifluoromethyl)-*meso*-triarylcorrole derivatives are sterically hindered species, with strongly saddled geometries and very short F···F nonbonded contacts.

2. The CF_3 groups appear as quartets in the ^{19}F NMR spectra, with unexpectedly large $^5J_{FF}$ coupling constants of about 14 Hz, apparently a manifestation of the highly crowded structure.

3. Not surprisingly, the eight CF_3 groups together exert a massive influence on the redox potentials of the copper corrole core. Thus, the $E_{1/2ox}$ of Cu[$(CF_3)_8$TPC] is a full half of a volt above that of Cu(TPC) and a quarter of a volt above that of either Cu(Br_8TPC) or Cu(F_8TPC).

4. More intriguingly, the β CF_3 groups also intensify the influence of the meso aryl substituents on the redox potentials, relative to the other Cu[Y_8T(*p*-XP)C] series, where Y = H, F, and Br.

5. The Cu[$(CF_3)_8$T(*p*-XP)C] complexes exhibit the most red-shifted optical spectra of any series of metallocorroles synthesized to date. Thus, between Cu(TPC) and Cu[$(CF_3)_8$T(*p*-MeO-P)C], the Soret maximum shifts by nearly 100 nm.

It is clear that fluorinated and particularly perfluoroalkylated corroles exhibit a concatenation of remarkable physical and chemical properties. The copper β-octakis(trifluoromethyl)corrole complexes may be viewed as new exemplars for appreciating ligand substituent effects in metallotetrapyrrole complexes and, by extension, in transition metal complexes in general. Efforts are under way to exploit these compounds as novel reagents, catalysts and functional materials. Toward this end, syntheses of additional families of fluorinated corroles are being actively pursued in our laboratory.

Experimental Section

Materials. All reagents and solvents were used as purchased, except pyrrole and dimethylformamide (DMF), which were predried and distilled from CaH_2 at reduced pressure. Silica gel 60 (0.04−0.063 mm particle size; 230−400 mesh, Merck) was used for flash chromatography. Silica gel 60 preparative thin-layer chromatographic plates (20 × 20 cm; 0.5-mm-thick, Merck) were used for further purification of the trifluoromethylated corroles.

Instrumentation. Ultraviolet−visible spectra were recorded on an HP 8453 spectrophotometer using dichloromethane as solvent. Cyclic voltammetry was performed with an EG&G Model 263A potentiostat having a three-electrode system consisting of a glassy carbon working electrode, a platinum wire counter electrode, and a saturated calomel reference electrode (SCE). Tetra(*n*-butyl)ammonium perchlorate (TBAP), recrystallized from 95% ethanol and dried in a desiccator for at least one week, was used as a supporting electrolyte. Dichloromethane, distilled and stored over 4 Å molecular sieves, was used as solvent. The reference electrode was separated from bulk solution by a fritted-glass bridge filled with the solvent/supporting electrolyte mixture. All potentials were referenced to the SCE. Pure argon was bubbled through the sample solutions for at least 2 min before the experiments were run. The argon stream was allowed to flow above the surface of the solutions while these experiments were performed, thus creating an argon blanket to exclude air from these solutions. NMR spectra were recorded on a Mercury Plus Varian spectrometer (400 MHz for ^1H and 376 MHz for ^{19}F) at room temperature in chloroform-*d*. Proton chemical shifts (δ) in parts per million were referenced to residual chloroform (δ = 7.2 ppm). Fluorine-19 chemical shifts (δ) in parts per million were referenced to 2,2,2-trifluoroethanol-d_3 (δ = −77.8 ppm). MALDI-TOF mass spectra were recorded on a Waters Micromass MALDI micro MX Mass Spectrometer using α-cyano-4-hydroxycinnamic acid as matrix.

Synthesis of Corrole Starting Materials. Free base *meso*-triphenylcorrole, *meso*-tris(4-fluorophenyl)corrole, *meso*-tris(4-methylphenyl)corrole, and *meso*-tris(4-methoxyphenyl)corrole were synthesized as previously described.[9] Copper triarylcorroles and their β-octabromo derivatives were also synthesized as before.[9] The new trifluoromethylated copper(III) corroles were prepared according to the same procedure reported for β-octakis(trifluoromethyl)porphyrins.[12]

General Procedure for the Synthesis of Trifluoromethylated Corroles. The synthetic procedures were identical for all four complexes with the following exceptions. The palladium catalyst and triphenylarsine were not needed for synthesizing the Cu[$(CF_3)_8$T(*p*-FP)C] complex, and the exact compositions of the eluents in the final chromatography were slightly different for the different complexes, as noted in detail below. In other respects, the following general procedure applied to all syntheses.

Copper octabromocorrole (40 mg), 5 mol % tris(dibenzylideneacetone)-dipalladium(0)-chloroform (Fluka), 40 mol % triphenylarsine (Aldrich), and 42 equiv of copper(I) iodide (Aldrich) were introduced into a 25 mL three-necked round-bottomed flask equipped with a magnetic stirring bar and a reflux condenser. Dry DMF (5 mL) was added to the solids while flushing the system simultaneously with argon. After stirring and degassing the reaction mixture for 5 min, 42 equiv of methyl 2,2-difluoro-2-(fluorosulfonyl)acetate was added to it. The suspension so produced was stirred under argon for 60−80 min at 100 °C. The reaction was monitored by UV−vis spectroscopy and TLC. After complete consumption of the copper corrole starting material, the reaction mixture was cooled to room temperature, diluted with dichloromethane, and filtered. The filtrate was washed three times with distilled water, and the organic phase was dried over anhydrous sodium sulfate. After filtration and evaporation of the organic phase, the residue obtained was chromatographed on a silica gel column with (varying ratios of) an *n*-hexane/dichloromethane mixture as an eluent to give the trifluoromethylated corrole as the first eluate. The latter was dried and purified further by preparative TLC on glass-supported silica plates. Details of the individual syntheses are given below.

Copper 2,3,7,8,12,13,17,18-Octakis(trifluoromethyl)-5,10,15-triphenylcorrole. The reaction was complete after 60 min. The brown residue obtained after workup was chromatographed on a silica gel column with 37:3 hexane/dichloromethane as eluent to give the corrole product as the first brown eluate. This was dried and purified further by preparative TLC (eluent: 7:3 hexane/CH_2Cl_2) to yield the pure corrole as the second brown band. Yield: 5 mg (13.5%). R_f (3:2 hexane/CH_2Cl_2) = 0.42. UV−vis (CH_2Cl_2), λ_{max} (nm), [(log ε (M^{-1} cm^{-1})]: 459 (4.65), 743 (3.70). ^1H NMR: δ 7.87−7.82 (t, J = 7.2 Hz, 1H, 10-*p*, Ph); 7.82−7.76 (d, J = 7.6 Hz, 2H, 10-*o*, Ph); 7.75−7.57 (m, 6H, 5,15-*o* and -*p*, Ph); 7.53−7.48 (t, J = 7.2 Hz, 2H, 10-*m*, Ph); 7.48−7.36 (t, J = 8 Hz, 4H, 5,15-*m*, Ph). ^{19}F NMR: δ −50.78 (q, J = 14.3 Hz, 6F); −51.39 (q, J = 12.0 Hz, 6F); −51.47 (q, J = 14.3 Hz, 6F); −55.11 (q, J = 12.0 Hz, 6F). MS (MALDI-TOF, major isotopomer): M^+ = 1130.33 (exptl), 1130.02 (calcd). Elem anal.: 47.28% C (calcd 47.78%), 1.76% H (calcd 1.34%), 4.89% N (calcd 4.95%).

Copper 2,3,7,8,12,13,17,18-Octakis(trifluoromethyl)-5,10,15-tris(4-fluorophenyl)corrole. Tris(dibenzylideneacetone)dipalladium(0)-chloroform and triphenylarsine were not used in this reaction. The reaction was complete after 85 min. The brown residue

obtained after workup was chromatographed on a silica gel column with 13:3 hexane/dichloromethane as eluent to give the corrole product as the first brown eluate. This was dried and purified further by preparative TLC (eluent: 7:3 hexane/CH_2Cl_2) to yield the pure corrole as the second brown band. Yield: 8.8 mg (23.7%). R_f (4:1 hexane/CH_2Cl_2) = 0.138. UV−vis (CH_2Cl_2), λ_{max} (nm), [(log ε (M^{-1} cm^{-1})]: 462 (5.05), 749 (4.12). ^{1}H NMR: δ 7.84−7.74 (dd, J = 4.8 Hz, 2H, 10-*o* or -*m*, Ph); 7.63 (s, 5,15-*o* or -*m*, Ph, 4H); 7.20 (t, J = 8.8 Hz, 2H, 10-*o* or -*m*, Ph); 7.15 (t, J = 8.4 Hz, 4H, 5,15-*o* or -*m*, Ph). ^{19}F NMR: δ −50.69 (q, J = 15.8 Hz, 6F), −51.20 to −51.45 (m, 12F), −55.13 (q, J = 13.2 Hz, 6F), −104.0 (s, 1F), −107.2 (s, 2F). MS (MALDI-TOF, major isotopomer): M^+ = 1183.95 (exptl), 1183.99 (calcd). Elem anal.: 46.31% C (calcd 45.61%), 1.70% H (calcd 1.02%), 4.40% N (calcd 4.73%).

Copper 2,3,7,8,12,13,17,18-Octakis(trifluoromethyl)-5,10,15-tris(4-methylphenyl)corrole. The reaction was complete after 80 min. The brown residue obtained after workup was chromatographed on a silica gel column with 37:3 hexane/dichloromethane as eluent to give the corrole product as the first brown eluate. This was dried and purified further by preparative TLC (eluent: 7:3 hexane/CH_2Cl_2) to yield the pure corrole as the first brown band. Yield: 9.4 mg (25.3%). R_f (3:2 hexane/CH_2Cl_2) = 0.467. UV−vis (CH_2Cl_2), λ_{max} (nm), [(log ε (M^{-1} cm^{-1})]: 383 (3.76), 471 (4.49), 773 (3.56). ^{1}H NMR: δ 7.69 (d, J = 7.6 Hz, 2H, 10-*o* or -*m*, Ph); 7.55 (d, J = 6.0 Hz, 4H, 5,15-*o* or -*m*, Ph); 7.30 (d, J = 8.0 Hz, 2H, 10-*o* or -*m*, Ph); 7.25 (d, J = 7.6 Hz, 4H, 5,15-*o* or -*m*, Ph); 2.43 (s, 6H, 5,15-*p*-CH_3, Ph); 2.32 (s, 3H, 10-*p*-CH_3, Ph). ^{19}F NMR: δ −50.84 (q, J = 14.3 Hz, 6F); −51.21 (q, J = 10.5 Hz, 6F); −51.27 (q, J = 14.6 Hz, 6F); −55.09 (q, J = 12.8 Hz, 6F). MS (MALDI-TOF, major isotopomer): M^+ = 1171.96 (exptl), 1172.07 (calcd). Elem anal.: 50.34% C (calcd 49.14%), 2.25% H (calcd 1.80%), 4.58% N (calcd 4.78%).

Copper 2,3,7,8,12,13,17,18-Octakis(trifluoromethyl)-5,10,15-tris(4-methoxyphenyl)corrole. The reaction was complete after 80 min. The red residue obtained after workup was chromatographed on a silica gel column with 13:7 hexane/dichloromethane as eluent to give the corrole as the first red eluate. This was dried and purified further by preparative TLC (eluent: 1:1 hexane/CH_2Cl_2) to yield the pure corrole as the first red band. Yield: 15 mg (40%). R_f (3:2 hexane/CH_2Cl_2) = 0.13. UV−vis (CH_2Cl_2), λ_{max} (nm), [(log ε (M^{-1} cm^{-1})]: 384 (3.04), 507 (3.77), 803 (3.07). ^{1}H NMR: δ 7.77 (d, J = 8.4 Hz, 2H, 10-*o* or -*m*, Ph); 7.64 (d, J = 8.0 Hz, 4H, 5,15- *o* or *m*, Ph); 7.03 (d, J = 9.2 Hz, 2H, 10-*o* or *m*, Ph); 6.97 (d, J = 8.4 Hz, 4H, 5,15-*o* or -*m*, Ph); 3.91 (s, 9H, 5,10,15-*p*-OCH_3, Ph). ^{19}F NMR: δ −51.05 (q, J = 13.2 Hz, 6F); −51.13 to −51.35 (m, 12F); −55.09 (q, J = 13.2 Hz, 6F). MS (MALDI-TOF, major isotopomer): M^+ = 1219.85 (exptl), 1220.05 (calcd). Elem anal.: 46.91% C (47.21% calcd), 1.83% H (calcd 1.73%), 4.59% N (calcd 4.59%).

DFT Calculations. All DFT calculations were carried out using the ADF 2006 program system,[20] the OLYP[24] exchange-correlation functional, an all-electron STO-TZP basis set, a fine mesh for numerical calculations of the matrix elements, and adequately tight criteria for geometry optimizations. A spin-unrestricted formalism was used throughout.

Acknowledgment. This work was supported by the Research Council of Norway. A.G. thanks Professors Paul A. Deck (Virginia Tech), Steven H. Strauss (Colorado State University), and Richard D. Chambers (Durham, U.K.) for helpful correspondence.

Supporting Information Available: Analytical details (27 pages). This material is available free of charge via the Internet at http://pubs.acs.org.

IC801101K